Research Article

Guoyuan Li, Hui Tian, Qiang Li, Siwei Shan*, Jing Zhao*, Tao Li*

Raw Materials and Technological Choices: Case Study of Neolithic Black Pottery From the Middle Yangtze River Valley of China

https://doi.org/10.1515/opar-2024-0025
received July 7, 2023; accepted December 19, 2024

Abstract: Neolithic black pottery from continental Eurasia has attracted scholarly interest since the 1930s, yet its diverse production and use remains poorly understood. This study examined 165 black pottery sherds from Fenghuangzui, a walled town in the middle Yangtze River valley of China, to investigate raw materials and technological choices during the Upper Qujialing (5300–4500 cal BP) and Shijiahe (4500–4200 cal BP) periods. Raman analysis confirms that carbon black was the sole colorant, formed through the absorption of carbon particles. Microscopic examinations categorized 104 fine-paste sherds into 4 sub-groups based on surface texture, identifying 3 clay sources (AA, BB, and BB*) through chemical analysis. AA and BB were the primary sources during both periods, while BB and BB* were preferred in the Shijiahe period for higher-quality serving and drinking vessels linked to feasting. Thin-section petrography and thermal expansion curves indicate the use of local raw materials and firing temperatures of 820–920°C. The consistent clay sources and firing conditions suggest stable practices, while the correlation between certain clay sources and finer pots indicates the potter's adaptability to specific needs, reflecting the active role of Fenghuangzui inhabitants in socio-political events during the Shijiahe period.

Keywords: Fenghuangzui, Neolithic black pottery, chemical composition, thin-section petrography, technological choice

1 Introduction

Since the 1930s, Neolithic black pottery unearthed across continental Eurasia has drawn considerable scholarly attention due to its unique or distinct color, texture, and use. The functional interpretations or technological understanding of Neolithic black pottery have been reported for, for example, Greece (e.g., Childe, 1937; Holmberg, 1964; Oikonomou et al., 2012), China (e.g., An, 1979, 1988; Lu et al., 2011a, b; Wang et al., 2023),

*** Corresponding author: Siwei Shan,** Department of Archaeology, School of History, Wuhan University, Wuhan, 430072, China; Archaeological Institute for Yangtze Civilization (AIYC), Wuhan University, Wuhan, 430072, China, e-mail: swshan@whu.edu.cn
*** Corresponding author: Jing Zhao,** Shanghai Institute of Ceramics, Chinese Academy of Sciences, Shanghai, 200050, China, e-mail: zhaojing@mail.sic.ac.cn
*** Corresponding author: Tao Li,** Department of Archaeology, School of History, Wuhan University, Wuhan, 430072, China; Laboratory for Comparative Archaeology, Wuhan University, Wuhan, 430072, China; Archaeological Institute for Yangtze Civilization (AIYC), Wuhan University, Wuhan, 430072, China, e-mail: tao-li@live.com
Guoyuan Li: Department of Archaeology, School of History, Wuhan University, Wuhan, 430072, China; Laboratory for Comparative Archaeology, Wuhan University, Wuhan, 430072, China
Hui Tian: The Fenghuangzui Conservation Center, Xiangyang, 441129, China
Qiang Li: Shanghai Institute of Ceramics, Chinese Academy of Sciences, Shanghai, 200050, China
ORCID: Tao Li 0000-0002-1390-6309

Macedonia and Thrace (Tsurev, 2022; Yiouni, 2001), Denmark (Trąbska et al., 2011), Poland (Łaciak et al., 2019), and Italy (Fanti et al., 2024). The different ways of producing pots with a black surface (or black surfaces) and the diverse contexts of their circulation and use have significantly enhanced our understanding of Neolithic populations' evolving minds and concepts (of, say, the distinction between "us" and "otherness," the value system, and the increasingly complicated interpersonal social or economic ties).

In China, black pottery was first reported in the early 1930s for the Longshan culture (4600–4000 cal BP), a Late Neolithic culture characterized by its production and use of finely crafted black pots in Shandong Province of the lower Yellow River valley (Fu et al., 1934; Wu, 1930). Many typological and technological studies have been conducted to understand the production, distribution, and use of the Longshan culture black pottery ever since then (e.g., Druc et al., 2018; Du, 1982; Fan et al., 2005; Lu, 2021; Lu et al., 2011b; Qiu et al., 2001; Shen et al., 2008; Underhill, 1991; Wu, 1938; Zhong, 1989). Far south of the Shandong Province, archaeological excavations in the lower Yangtze River valley yielded fiber-tempered black pottery dating to some 7,000 years ago at the sites of Hemudu and Kuahuqiao (e.g., Fan, 2015; Li et al., 1979). People attempted to produce and use black pottery in this area. The Tangjiagang (6900–5900 cal BP), Daxi (5900–5300 cal BP), and Upper Qujialing (5300–4500 cal BP) cultures in the middle Yangtze River valley are also featured by their intensive use of black pottery (Fan, 2015). However, Neolithic black pottery from the middle Yangtze River valley has been poorly understood compared to the lower Yellow and lower Yangtze River valleys.

Regional specialists, ourselves included, have observed significant variations in the macroscopic characteristics of black pottery in the middle Yangtze River valley, such as paste color, texture, shape, and contextual use. Inspired by the research of Izumi Shimada and Ursel Wagner, who studied black pottery in Peru, we concur with their statement that "Not all 'black' pottery was produced in the same manner just as their social and symbolic uses and reasons for production varied a good deal" (Shimada & Wagner, 2019, p. 133). Similarly, we believe that the significant variations among the Neolithic black pottery in our region suggest not only the exploitation of diverse raw materials (clay sources and tempering materials) but also, more importantly, the many ways that people conceptualized their minds and practiced their deeds to meet functional requirements and cultural and social needs. Nevertheless, the existing data mainly focus on black pots' aesthetically pleasing color and firing techniques (e.g., Li & Huang, 1985; Xiao et al., 2022), with limited insights into how and why different raw materials were used to make various black pottery.

To most archaeologists or ceramic specialists in the region, "black pottery" refers to pottery that is "black" in color, but the generic term, "black pottery," masks the great diversity and complexity in pottery's color, hues, textures, and other attributes. For example, some black pottery has a black surface but is gray or reddish at the core (Fan, 2015; Lu et al., 2013). Some pots are only black on the exterior surface, while others show a black finish on the interior surface (Li & Huang, 1985). Some pots have a black coating or slip (e.g., Cui et al., 2017; Longacre et al., 2000; Lu et al., 2011a). In addition, black pots often have various hues and textures (Zhong, 1989), and they seem to differ in shaping and forming techniques, surface treatment, and raw materials (Fan et al., 2005; Lu, 2021). Also, different types of potteries may have different functions of use. Not only are there elaborate black vessels that may be used as prestige goods (such as the Longshan culture eggshell black pottery), but there are also utilitarian black pots for daily use. Last, black pots were recovered in various contexts (e.g., as grave goods, household trash, and remains related to feasts), possibly indicating different social functions or symbolic meanings as demonstrated elsewhere (Nam et al., 2020; Shimada & Wagner, 2019). In this article, we define a "black" pot from a broader definition; that is, pottery is considered "black" if it has a wholly "black" exterior or interior surface. Pottery with black spots or stains from soot or firing, which is relatively easy to identify by the naked eye, is excluded from this definition.

Beginning in August 2020, archaeological excavations at the site of Fenghuangzui in the Xiangyang City of Hubei Province, central China, have unearthed substantial amounts of black pottery showing a noticeable diversity in texture, hue, and surface treatment. The site was a regional center occupied mainly from the Upper Qujialing period to the Meishan period, radiocarbon dated between 5300 and 3900 cal BP (Li et al., 2022). Our article here focuses on black pottery dating to the Upper Qujialing (5300–4500 cal BP) and Shijiahe (4500–4200 cal BP) periods, the most prosperous periods for the development of the Fenghuangzui site. A multi-analytical approach – combining Raman spectroscopy, microscopic examination, chemical compositional analysis, thin-section petrography, and thermal expansion method – was applied to a sample of 165

black pottery sherds unearthed from Fenghuangzui to help understand the raw materials and technological choices in making black pots at the site. Unlike previous studies focusing on the manufacturing or firing technique, we pay great attention to how flexibly the Neolithic potters selected raw materials to meet the technical, functional, and social demands at the site of Fenghuangzui. The study results provide clues to the different ways of producing and using black pottery, thus advancing the current understanding of black pottery production and use in the Neolithic middle Yangtze River valley.

2 Neolithic Black Pottery in the Middle Yangtze River Valley: An Overview

The middle Yangtze River valley refers to the Jianghan Plain, Dongting Lake Plain, and neighboring areas at the heart of China. Back in Neolithic times, distinct yet relatively isolated regional patterns of cultural traditions had been well established in the region, making it a unique geographic area for understanding how patterns of Chinese culture took shape into its diversity and unity (Meng, 1997). This region has a long cultural tradition of making and using black pottery. Archaeological discoveries of Neolithic black pottery are abundant here, demonstrating technological and stylistic changes over time. Based on the widely accepted chronology of archaeological cultures in the middle Yangtze River valley (Meng, 1997) and also on the new insights into the regional cultural chronology offered by Shan (2018, 2021), this article presents a brief overview of Neolithic black pottery from the three core areas of the middle Yangtze River valley – the Dongting Lake region, the Xiajiang River region, and the Handong region. The archaeological cultures of our concern and their spatial and temporal distributions are detailed in Table 1.

Before the broad appearance of black pottery in the middle Yangtze River valley, the region was dominated by fiber-tempered and sand-tempered red pottery, often with a black core on the pot's cross-section or with a red slip. Black pottery – mostly fine-paste but also fiber-tempered or sand-tempered – began to be produced and used in the middle Yangtze River valley 7,000 years ago (Fan, 2015). A few black pottery sherds were collected from the Late Chengbeixi and Lower Zaoshi cultures (Hubei, 2001; Wang & Zhang, 1993). In the subsequent Tangjiagang, Liulinxi, and Bianfan cultural periods (6900–5900 cal BP), black pottery was used more often than before. Many excavation reports refer to them as "jianghei tao" (dark-colored pottery), and at each site, dark-colored pots were estimated to account for 1–5% of all sherds (Meng, 1997; Wang & Zhou, 2003; Zhang, 1987). While black pottery was not insignificant by this time, most potteries still showed a reddish color on their surface(s).

The Daxi culture emerged as a dominant culture in the middle Yangtze River valley between 5900 and 5300 cal BP, and its materials were widely distributed across the Dongting Lake and Xiajiang regions. The Daxi

Table 1: Chronology of regional cultures in the three core areas of the Neolithic middle Yangtze River valley (Shan et al., 2021)

Dates in cal BP	Distribution area	Characteristic regional cultures
8500–7800	Dongting Lake region	Pengtoushan culture
7800–6900	Dongting Lake region	Lower Zaoshi culture
	Xiajiang River region	Chengbeixi culture
6900–5900	Dongting Lake region	Tangjiagang culture
	Xiajiang River region	Liulinxi culture
	Handong region	Bianfan culture
5900–5300	Dongting Lake region	Daxi culture
	Xiajiang River region	
	Handong region	Youziling culture
		Lower Qujialing culture
5300–4500	Entire middle Yangtze River valley	Upper Qujialing culture
4500–4200	Entire middle Yangtze River valley	Shijiahe culture
4200–3900	Entire middle Yangtze River valley	Meishan culture

culture was subdivided into the early and later phases. Black pottery's proportion increased to 5–15% in the early phase. By the later phase, black pottery increased significantly in absolute and relative terms, and 20–40% of the sherds were black (Zhang et al., 1982). "Real" black pottery, with a black finish and a black body/core, began to be produced and used at this time (Fan, 2015). Another distinct feature of the Daxi pottery is that the pottery sometimes had a black color on the interior surface but a red color on the exterior surface, the cultural or symbolic meaning of which has remained unexplored. Technically, the black color on the interior surfaces of Daxi pottery was made on purpose, probably through the carbon smudging when the pots came out of the kiln (Li & Huang, 1985). Alternatively, it could have resulted from inadequate oxidation in the firing of the pottery through the absorption and penetration of carbon particles (Zhang et al., 1982).

Like the Dongting Lake and Xiajiang regions, the Handong region was also characterized by the production and use of black pottery. It outnumbered other areas of the middle Yangtze River valley in the quantity and proportion of black pottery and demonstrated the capability of producing "real" black pots much earlier (Fan, 2015). In this region, black pottery accounted for 20–40% of the pottery assemblage during the Youziling cultural period (5900–5500 cal BP) (Li, 1994). In addition to utilitarian use, black potteries were used as grave goods, and they had a significantly higher probability (ca. 80%) of being found in Lower Qujialing culture burials than other colors (Li, 1994). The black pottery of the Daxi cultural period received more attention among researchers. For example, Li and Huang (1985) investigated the firing technique of black pottery, focusing primarily on the carbon smudging of the Daxi pottery; Fan (2015), also focusing on the Daxi culture pottery, investigated the impermeability of black pottery in the Neolithic middle Yangtze River valley.

The production and use of black pottery peaked during the Late Daxi and Lower Qujialing cultural periods, and it continued into the Upper Qujialing and Shijiahe cultural periods, dating between 5300 and 4200 cal BP. However, black pottery decreased in importance in some areas, possibly resulting from the advance in firing technology, the functional demands for harder and more durable gray pottery, and/or the increasing preference for red pottery. Notably, black pottery decreased in proportion in the core area of the Shijiahe culture, which is characterized by the extensive and intensive production and use of red pottery artifacts (The Jingzhou Museum, Peking University, Hubei Provincial Institute of Cultural Relics and Archaeology, The Shijiahe Archaeological Team, 2011). It is interesting to notice that at the Fenghuangzui site, far beyond the core area of the Upper Qujialing and Shijiahe cultures, black pottery still significantly contributes to the pottery assemblages during the Upper Qujialing and Shijiahe cultural periods.

In summary, Neolithic black pottery in the middle Yangtze River valley is abundant and has attracted attention among regional specialists. However, Neolithic black pottery from the region has been poorly understood. Multi-analytical approaches have not been employed to investigate the production, circulation, and use of Neolithic black pottery in the region.

3 Materials and Methods

3.1 The Fenghuangzui Site and the Sherd Sampling

The site of Fenghuangzui, 15 ha in size, is located in the middle Hanshui River valley and on the southern edge of the Nanyang Basin in central China. A Late Neolithic walled settlement (or a "town"), occupied mainly through the Upper Qujialing period to the Meishan period, was identified at the site. Among the 20 or so Neolithic walled towns discovered thus far in the middle Yangtze River valley (Shan et al., 2021), the walled town at Fenghuangzui stands out as the most distant from the core areas of the Upper Qujialing and Shijiahe cultures.

Beginning in August 2020, archaeological excavations have been conducted within and around the Neolithic walled town at Fenghuangzui, revealing impressive features such as the enclosing wall, moat, higher-status households, burials, and impressively large ash pits containing different kinds of artifactual assemblages (H13 and H17, e.g.). Large quantities of artifacts made from pottery, stone, jade, and turquoise

have also been excavated (Li et al., 2022). Geographically, the site is located in a key region that connects North and South China. Archaeological excavations at the site since August 2020 have yielded artifacts indicative of cultural contact with, for example, the Longshan culture in Shandong Province of East China. In more than one aspect, the site is significant for understanding the development of social complexity, regional settlement patterns, household and community identity, craft production, and cultural communications, especially in the water-abundant regions of Late Neolithic China.

Figure 1 shows the geographic location of Fenghuangzui in the middle Yangtze River valley and Figure 2 shows the structure and major components of the walled settlement discovered at Fenghuangzui. Since October 2022, probing surveys at and around the site have revealed more details of the walled town's structures. Full information will be published in another article.

Figure 1: (a) The map of China and (b) the locations of 19 Neolithic walled towns in the middle Yangtze River valley (1 = FHZ, shortened for Fenghuanzgui. See Supplementary Information for details of the other 18 walled towns).

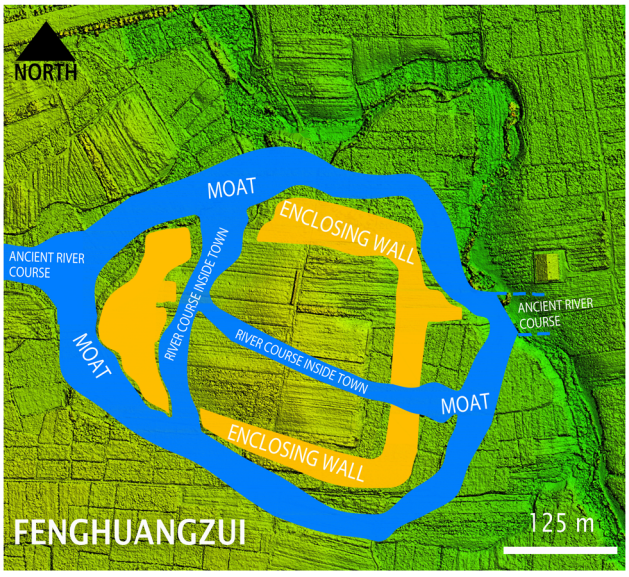

Figure 2: The structure and major components of the walled town revealed at Fenghuangzui.

The present article focused on three recently excavated ash pits (H13, H17, and H89), a few meters apart from one another, at the site (see Figure 3 for restored pottery assemblages from these pits). H13 is oval-shaped, measuring 6.6 m in long diameter, 2.1 m in short diameter, and 0.5 m in depth, with two layers most clearly identified. H17 is also oval, with a long diameter of 3.8 m, a short diameter of 2.8 m, and a depth of 0.8 m, consisting of ten recognizable layers. H89, intruded by H17, has an irregular shape, with a long diameter of

Figure 3: Restored pottery assemblages unearthed from ash pits H89, H17, and H13.

1.8 m, a short diameter of 0.8 m, and a depth of 0.2 m. Typological analysis suggests that H17 and H13 were used in the early and late stages of the Shijiahe period, respectively, and H89 was dated to the late stage of the Upper Qujialing period. That is, H89 is older than H17, followed by H13, by relative dating. AMS ^{14}C dating results suggest that H17 dates between 4500 and 4300 cal BP and H13 between 4400 and 4200 cal BP, which do not contradict the typological analysis. No radiocarbon dates are currently available for H89.

Based on our detailed count and classification of the sherds excavated from the pits (Figure 4), H13 contains 12,115 sherds, of which 5,836 (48%) are black or grayish-black, while H17 contains 12,808 sherds, of which 6,516 (51%) are black or grayish-black (Figure 4a). Most sherds are fine-paste or shell-tempered, while sand-tempered or fiber-tempered accounts for only a small proportion. Furthermore, Figure 4b shows that pottery was either decorated with a basket pattern (widely noticed for H13) or plain but burnished (most abundant in H17). Judging from identifiable vessel shapes and forms (Figure 4c), H17 contains more serving (e.g., *wan*-bowl, *bo*-bowl, *pan*-plate, and *dou*-stemmed bowl) and drinking (e.g., *bei*-cup and *hu*-jar) vessels. It seems likely that pottery deposited in H13 and H17 differ not only in the date of formation but also in their contextual uses (a topic we will return later). Compared to H13 and H17, H89 is a much smaller ash pit containing fewer sherds (n = 514), mostly fine-paste and plain. Black sherds account for 38% (n = 194) of the total sherds unearthed from H89.

Taking sherds from H13, H17, and H89 as the sherd pool, we selected a sample of 165 black pottery sherds, including 77 from H13, 65 from H17, and 23 from H89 (see sample details in Table 2). The selected sherds represent most (if not all) textures, surface treatments, and paste colors we have identified for the three ash pits. The sample selection is done with the naked eye, which may involve subjective judgments.

3.2 Methods and Instrumental Details

3.2.1 Raman Spectroscopy

Raman analysis was applied to the black pottery to understand the colorant materials. The confocal XploRA PLUS Raman microscope (Horiba Jobin Yvon, France) was used. Two excitations (532 and 785 nm) were tried to obtain the best Raman signals for the black color. Seven black sherd specimens (FHZ011, FHZ013, FHZ045, FHZ047, FHZ071, FHZ098, and FHZ137) were selected for Raman analysis because they demonstrated varying colors and hues. Raman analysis was conducted on each sherd specimen's surface and cross-section to identify the colorant. We chose to report Raman spectra of the black color for the surface. Raman spectra were recorded in wavenumber between 100 and 3,000 cm^{-1}, with spectra accuracy of 2 cm^{-1}. An optical microscope focused the laser on samples at 50× magnifications throughout the analysis. Background spectra of water and carbon dioxide are obtained in ambient air. Raman spectra presented here were smoothed without baseline correction.

3.2.2 Microscopic Examination

We used a handheld Dino-lite AM7915MZT microscope to help examine the (overall) microstructures of the 165 selected sherds at 50× magnifications. All sherds were water-cleaned and hand-polished with 1,500-mesh sandpaper to produce smooth cross-sections for better examination. We pay attention to the exterior and interior surfaces and the cross-section of each sherd. Microstructural characteristics of each sherd were photographed and recorded.

3.2.3 Chemical Compositional Analysis

The chemical compositions of the 165 selected sherds (see sample information in Supplementary Information) were obtained from a handheld X-ray fluorescence (hhXRF) analyzer. Furthermore, eight sherd specimens were also analyzed using benchtop X-ray fluorescence.

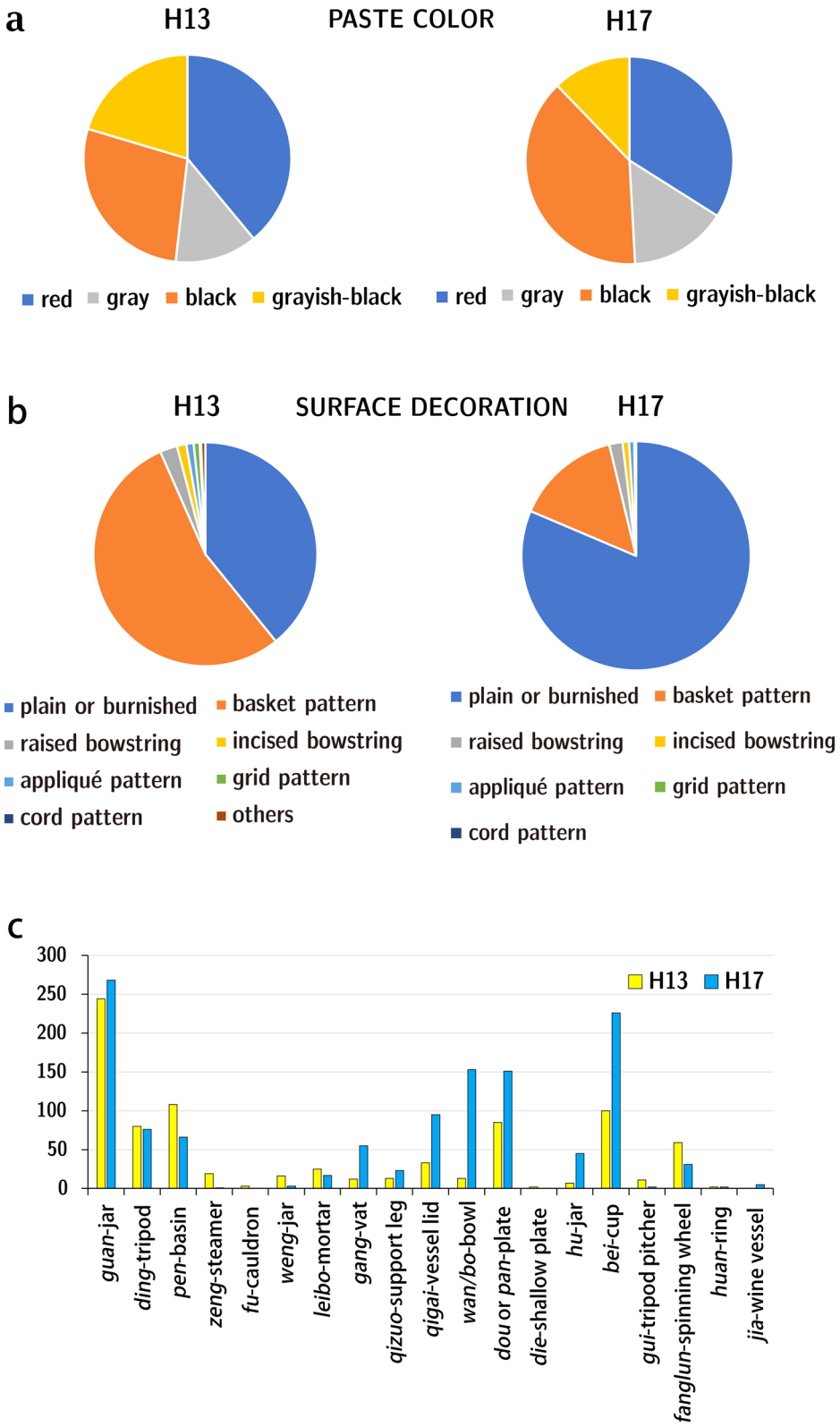

Figure 4: (a) Sherds' paste color and (b) decorations for H13 and H17 and (c) counts of sherds for different vessel forms (see details about the counts of sherds supporting Figure 4 in Supplementary Information).

Table 2: Details of the 165 black sherds unearthed from the site of Fenghuangzui

Ash pit	Texture	Decoration patterns					
		Basket pattern	Plain or burnished	Incised bowstring	Raised bowstring	Cord pattern	Grid pattern
H13 (*n* = 77)	Fine-paste	23	26	1			
	Shell-tempered	13	6				
	Sand-tempered	4	1			1	
	Fiber-tempered	2					
H17 (*n* = 65)	Fine-paste	11	31	1			1
	Shell-tempered	11	9				
	Sand-tempered	1					
H89 (*n* = 23)	Fine-paste		10				
	Shell-tempered		6				
	Sand-tempered		6		1		

3.2.3.1 Handheld X-ray Fluorescence Analyzer

A Thermo Fisher Scientific Niton XL3+ 950 handheld X-ray fluorescence analyzer was used to collect compositional data from the exterior and interior surfaces of the 165 sherd specimens. The hhXRF analyzer was equipped with a 50 kV X-ray tube (max. 50 kV, 100 μA, 2 W) with an Ag anode and a large drift detector with an active area of 7 mm^2 fitted with a polymer winder (MOXTEK AP 3.3 film), which provides superior X-ray transmission in the low-energy range down to the Mg Kα. The X-ray beam spot focusing on the sample was about 3 mm in diameter. The detection limits for analyzing sherds were based on a 120-s total analysis time (40 s for the high filter, 40 s for the low filter, and another 40 s for the main filter) in the soil mode.

The Niton XL3+ 950 handheld X-ray fluorescence analyzer is operated under a fundamental parameter (FP) calibration mode (performed at the factory). Our previous studies compared the patterns of chemical variations in sherds, which were tested by benchtop X-ray fluorescence analyzer (with the fusion method), inductively coupled plasma atomic emission spectroscopy, and Niton XL3+ 950 hhXRF analyzer (with an FP calibration mode). Although the chemical composition data obtained from the three methods varied in accuracy and precision, they all led to the same conclusion: sherds collected within the same residential area looked more alike in geochemical composition and tended to be grouped into the same compositional groups and, in the meanwhile, they are geochemically more different from pottery produced and consumed in other residential areas (Li, 2016). These patterned chemical variations help us understand how pottery may have been produced, distributed, and consumed. Our recent chemical analysis of ethnographic materials (clays and pottery) sampled from a relatively small spatial extent also strengthens our confidence in hhXRF data (Li et al., 2024).

We collected six hhXRF readings and calculated the average value for each sherd. Up to 33 elements were detected but most were excluded from further analysis due to their significant relative standard deviation. Data processing has been described in several of our previous studies (e.g., Ao et al., 2023; He et al., 2023; Li, 2020; Li et al., 2021), but a most complete and detailed description is presented in Li et al. (2022). The final compositional dataset consists of ten major, minor, and trace elements (zirconium, Zr; strontium, Sr; rubidium, Rb; zinc, Zn; iron, Fe; chromium, Cr; titanium, Ti; calcium, Ca; potassium, K; and barium, Ba), whose concentrations remain stable and show a relative error of less than 15%. Statistical analyses were performed with SYSTAT (Systat Software Inc, version 13).

3.2.3.2 Benchtop X-ray Fluorescence Analyzer

We also selected eight sherds – FHZ001, FHZ008, FHZ015, FHZ022, FHZ063, FHZ080, FHZ091, and FHZ102 – for benchtop XRF analysis on a PANalytical's Axios Max-Metals wavelength dispersive XRF spectrometer. Before the tests, all sherds were polished to ensure that their surfaces were smooth enough, and the black finish was removed entirely. We chose these eight sherd specimens because they show different microscopic structures and belong to different compositional groups according to the hhXRF data. It concerns us how the handheld XRF data are compatible with the benchtop XRF data. (We have recently tested 91 of the 104 fine-paste black pottery sherds with the benchtop X-ray fluorescence analyzer. The results, once again, well support the chemical groupings delineated by hhXRF. We will report these results in another article.)

3.2.4 Thin-Section Petrography

The eight sherds above were cut, mounted, polished, and prepared into thin slices of 30 μm (0.03 mm). Thin sections were examined under a Leica DMS1000 digital microscope, with 6×–300× magnifications. Mineral identification was carried out based on the optical properties of the mineral (such as cleavage, steak, interference color, and relief).

3.2.5 Thermal Expansion

We selected another sample of eight sherds (FHZ009, FHZ017, FHZ093, FHZ100, FHZ118, FHZ139, FHZ145, and FHZ147) and tested them with the thermal expansion method to determine their maximal firing temperatures.

These sherds are larger sherd fragments. They were selected to meet the sample size requirements for the thermal expansion method. The sherd specimens FHZ009 and FHZ118 cracked when dried and thus were excluded from the discussion.

4 Results

4.1 Raman Analysis of the Black Finish

Raman spectra of the black finish on the seven sherd specimens reveal the same spectral features, showing two broad Raman peaks at about 1,350 and 1,590 cm^{-1} (Figure 5). The two Raman peaks are characteristic of carbon black (C) (Bell et al., 1997), indicating that the black pottery's black exterior and/or interior surface is composed of carbon. The results are compatible with previous technical studies of Neolithic black pottery in the middle Yangtze River valley. For instance, Li and Huang (1985) argue that the Daxi pottery's black finish was formed through the absorption and penetration of carbon particles, either in the kiln or by post-firing treatment. It is beyond the scope of our article to discuss the mechanism of the formation of the black finish; however, we will return later to this topic when introducing the thermal expansion curves of the selected black pottery sherds.

4.2 Microscopic Examination

Microscopic observation was a powerful tool to reveal the variations in the pottery fabric's texture, paste color, and microstructures. The 165 black pottery sherds were grouped according to the presence/absence and type of

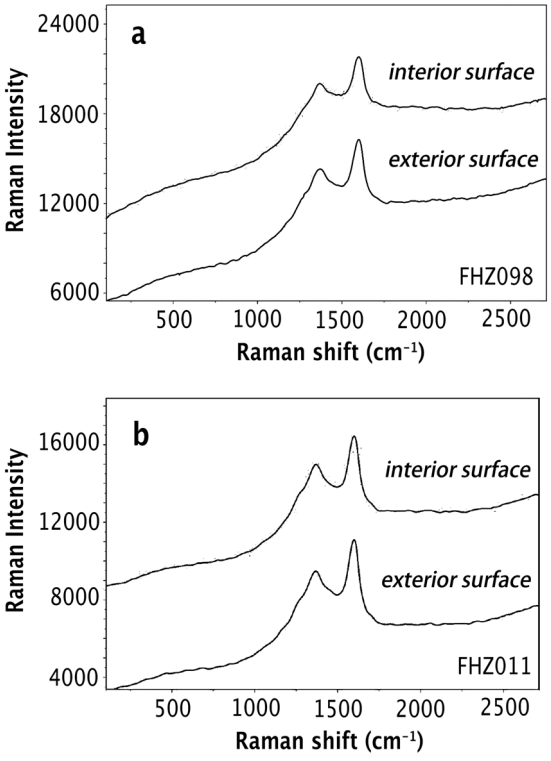

Figure 5: Raman analysis of the black finish on the exterior and interior surfaces. (a) FHZ098; (b) FHZ011.

inclusions (we did not distinguish between natural inclusions and artificially added inclusions). The fine-paste group consists of 104 sherds that contain immeasurable mineral particles and are, just as its name suggests, finely pasted; the coarse-paste (also referred to as sand-tempered in this work) group contains 14 sherds with identifiable mineral particles (mostly quartz and feldspar) of 0.1 mm or greater in diameter; the shell-tempered group contains 45 sherds with crushed shell residues; and the fiber-tempered group contains 2 sherds with many holes whose inner surfaces are attached with carbon particles.

Even within the same group of sherds, we noticed significant differences in texture. Our examination revealed substantial differences among the 104 fine-paste group sherds: some sherds show a "rough" surface with densely distributed white or transparent minerals of larger particle sizes (Figure 6a), while others are very "fine and smooth" on the surface, with fewer and smaller particles (Figure 6b). We went further by dividing the 104 sherds of the fine-paste group into 4 sub-groups: A (n = 57), A1 (n = 11), A1/B (n = 18), and B (n = 18). The microscopic images of the four sub-groups of sherds are shown in Supplementary Information.

Sub-groups A and B are easily distinguished, the former characterized by a rough and coarse surface (Figure 6a) while the latter by the finest and smoothest surface (Figure 6b). Sub-group A1 contains sherds that look more similar to, although not typical of, sub-group A. All other sherds were assigned to sub-group A1/B because they fall between A1 and B but are difficult to assign to either sub-group.

In short, from A to A1 to A1/B and then to B, the surface texture of the pottery sherds goes from rough to fine. Without a doubt, we subdivided the four sub-groups subjectively because the image resolution, the lighting, and the contaminants on the sherd's surface may mislead us in making a distinction. However, as we will show later, the sub-groups delineated above are supported by chemical compositional analysis.

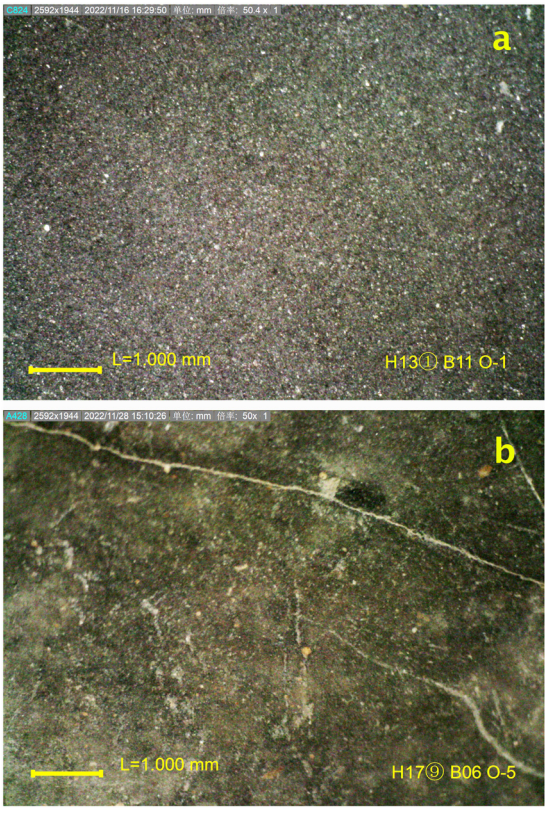

Figure 6: Macroscopic examination showing two extremely different textures among the black pottery sherds (a) coarse and rough characterizing sub-group A; (b) fine and smooth characterizing sub-group B.

4.3 Chemical Compositional Analysis

4.3.1 hhXRF Data

The hhXRF dataset consists of the chemical compositions of 10 elements (Zr, Sr, Rb, Zn, Fe, Cr, Ti, Ca, K, and Ba) for the 165 black pottery sherds. To minimize errors introduced by mineral inclusions or crushed shells, we focused on the 104 fine-paste sherds. Specifically, we compared the 104 fine-paste sherds representing the 4 sub-groups (A, A1, A1/B, and B) to explore variations in their chemical compositions and to examine

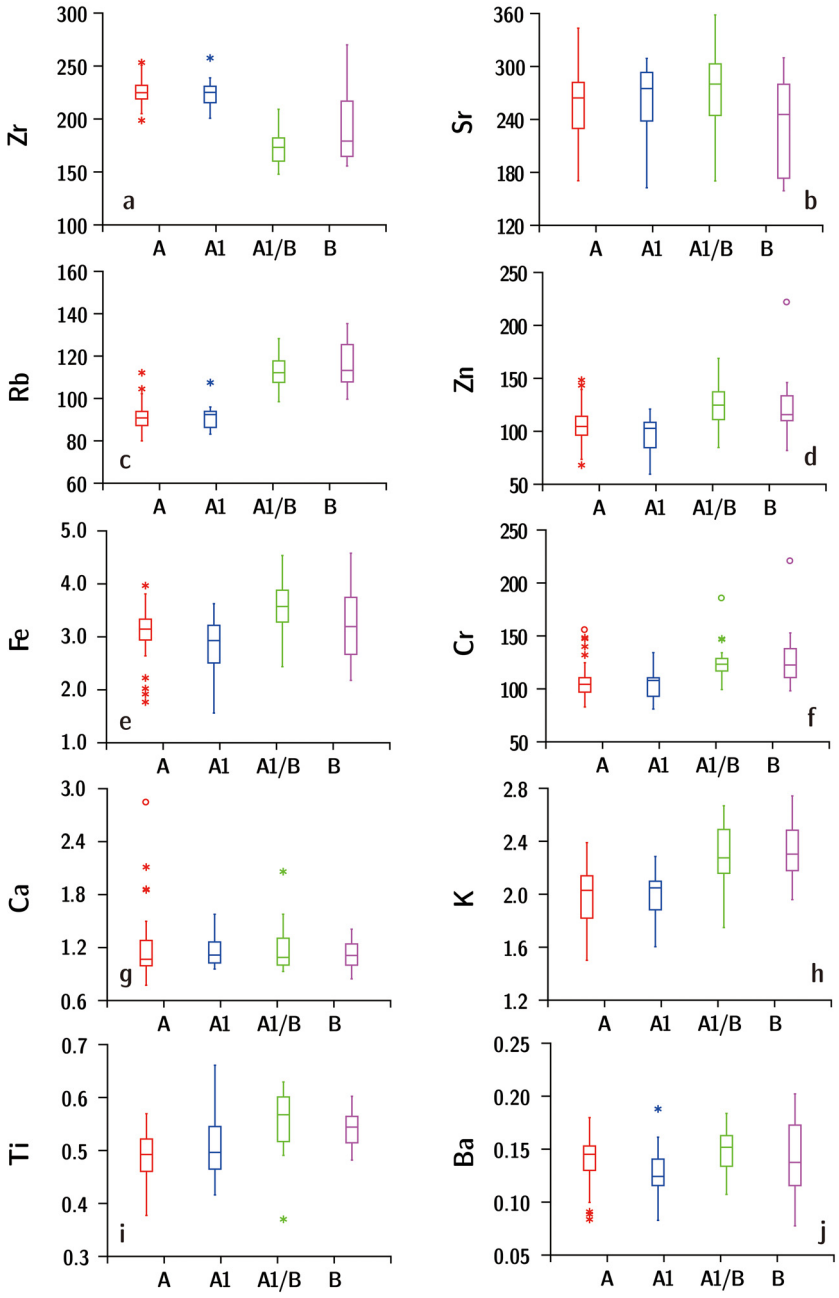

Figure 7: Comparisons of the 4 sub-groups of the 104 fine-paste sherds in their chemical composition (a) Zr; (b) Sr; (c) Rb; (d) Zn; (e) Fe; (f) Cr; (g) Ca; (h) K; (i) Ti; (j) Ba. Fe, Ca, K, Ti, and Ba, wt%; Zr, Rb, Sr, Zn, and Cr, ppm.

the correlation between classifications based on microscopic examinations and those based on chemical composition.

We notice in Figure 7 that the sherds of sub-groups A and A1 barely differ in chemical composition, as do those of sub-groups A1/B and B. Meanwhile, sub-groups A and A1 are distinguishable from sub-groups A1/B and B in Zr, Rb, Zn, Cr, K, and Ti concentrations. Thus, the sherds in sub-groups A and A1 differ from A1/B and B in texture and chemical composition. The concentrations of Zr and Rb serve as better indicators for distinguishing sub-groups A and A1 from A1/B and B. We produced the biplots using log-transformed concentrations of Zr and Rb; the results are shown in Figure 8(a)–(d).

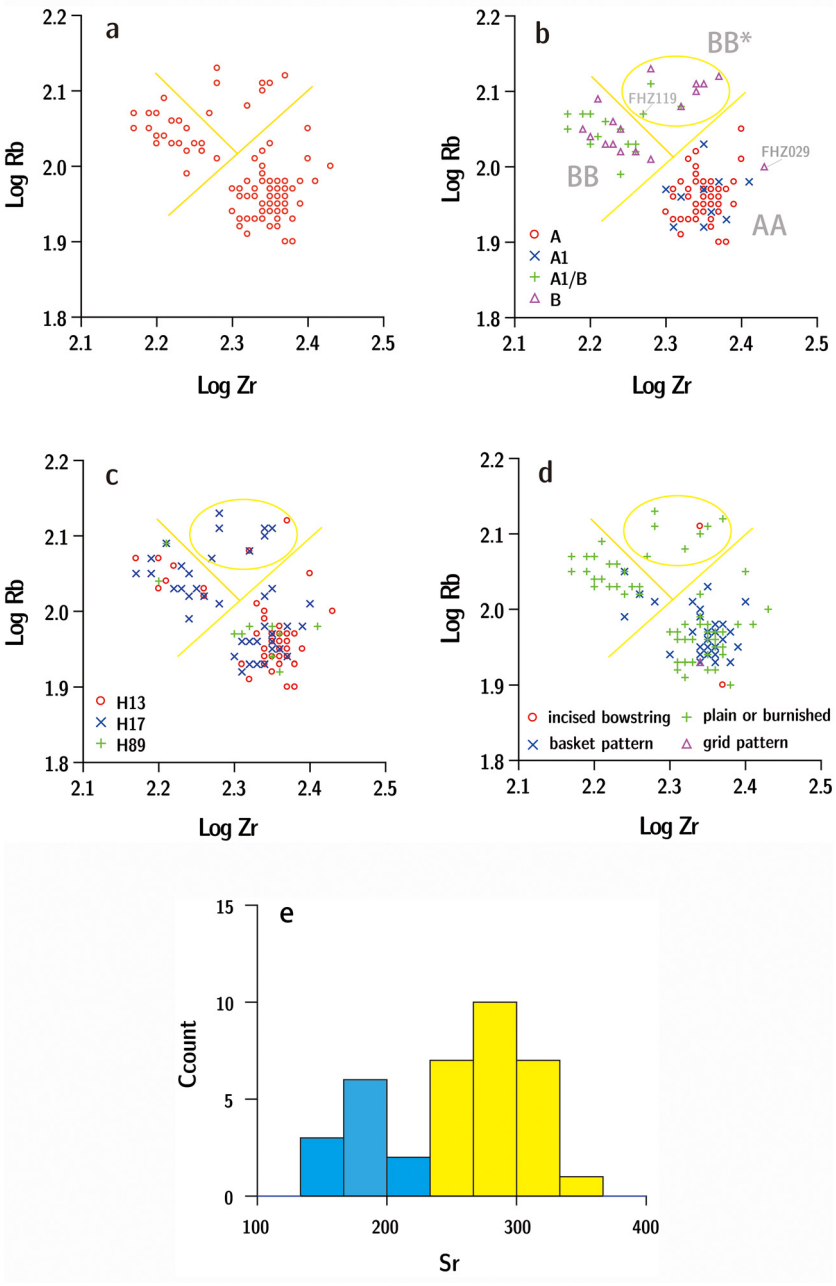

Figure 8: Biplots revealing subgroups among the 104 fine-paste sherds (a–d), and (e) the bimodal distribution of the concentration of Sr in group BB. Circles are drawn arbitrarily in b–d.

Based on the biplots in Figure 8(a)–(d), we made the following observations. First, the 104 sherd specimens are primarily divided into 2 groupings (Figure 8a), which are easily distinguishable from each other. Second, sub-groups A and A1 are indistinguishable, with high zirconium and low rubidium (Figure 8b). By contrast, sub-groups A1/B and B mostly overlap, showing low zirconium and high rubidium (Figure 8b).

In conjunction with the observations in Figure 7, we combined A and A1 to form a new group, AA (n = 68). A1/B and B form another new group, BB (n = 35). FHZ029 is an outlier whose microscopic observations are inconsistent with the composition. More experiments are needed to confirm why this inconsistency arises, but here we exclude FHZ029 from further analyses.

Third, the three ash pits (H13, H17, and H89) are indistinguishable from one another in terms of their pottery's chemical composition (Figure 8c). However, a distinction between (the newly defined) groups AA and BB is consistently noticed for all three pits. Furthermore, group BB is characterized by most sherds from H17, and most sherds from H13 and H89 are distributed in group AA.

Fourth, group AA is characterized by sherds with a basket pattern but also consists of plain or burnished sherds; in contrast, group BB consists mainly of plain or burnished sherds (Figure 8d).

Even within group BB, there are significant compositional variations. Nine sherds toward the upper-right corner are distinguished from the other sherds of group BB (Figure 8b). The compositional data of the nine samples also show low levels of Sr. The clear bimodal distribution of the concentration of Sr (Figure 8e) further confirms that sherds of group BB vary significantly in Sr. Relating the chemical compositional variations to microscopic examinations, we realized that the nine sherds are also distinct by their paste color, showing a light yellowish-gray color or an unusual color on the cross-section (Figures 9 and 10). We thus decided to define a new group, BB*, from group BB, which contains the nine sherds mentioned above. The remaining sherds were still assigned to group BB.

Based on the defined groups (AA, BB, and BB*) and their differences in the concentration of elements such as Zr, Rb, and Sr, we made a scatter plot of log-transformed zirconium (LogZr) vs the ratio of rubidium to strontium (Rb/Sr) for 103 sherds (FHZ029 excluded) to better show the compositional difference among the 3 groups. Furthermore, we applied the principal component analysis to the z-scored dataset consisting of the ten elements' concentrations of fine-paste sherds. The first three principal components account for most of the variance in the original compositional dataset, and biplots were produced using the first three PCA scores (PCA1: 33.6%; PCA2: 17.1%; PCA3: 11.0%). An 80% confidence ellipse is shown in each figure to help identify the likelihood that 1 sherd falls within or outside a compositional group.

We are 80% confident, given the plots in Figure 11, that the three new groups are indeed distinguishable from one another, especially when plotted with PCA1 and PCA2. In particular, group BB* is isolated from the other two. The compositional differences between groups AA and BB are well explained by the concentration of zirconium (Zr). Group BB* lies between groups AA and BB regarding the concentration of zirconium. Still, group BB* contains high rubidium and low strontium, resulting in a significantly higher rubidium/strontium ratio than groups AA and BB.

Once we include the shell-tempered, coarse-paste, and fiber-tempered sherds (Figure 12), we notice that these groups are indistinguishable from the fine-paste groups AA and BB in chemical composition; however, group BB*, once again, is noticeably distinguished from all others. In addition, a similar intragroup variation is noticed for the shell-tempered group, and the same patterning is noticed for groups AA and BB of the fine-paste group.

4.3.2 Benchtop X-ray Fluorescence Analysis

The handheld X-ray fluorescence analyzer can generate a chemical compositional dataset non-destructively and at low cost, and analysis of the hhXRF dataset revealed significant compositional variations among the sub-groups (either defined by texture, paste color, or chemical composition). How robust do the patterns we noticed for hhXRF data remain for compositional data generated by destructive, well-established analytical approaches? To answer this question, we collected eight sherd specimens from different sub-groups delineated within the fine-paste sherds and analyzed their chemical composition on a benchtop X-ray fluorescence analyzer. The results are shown in Figure 13 and Table 3.

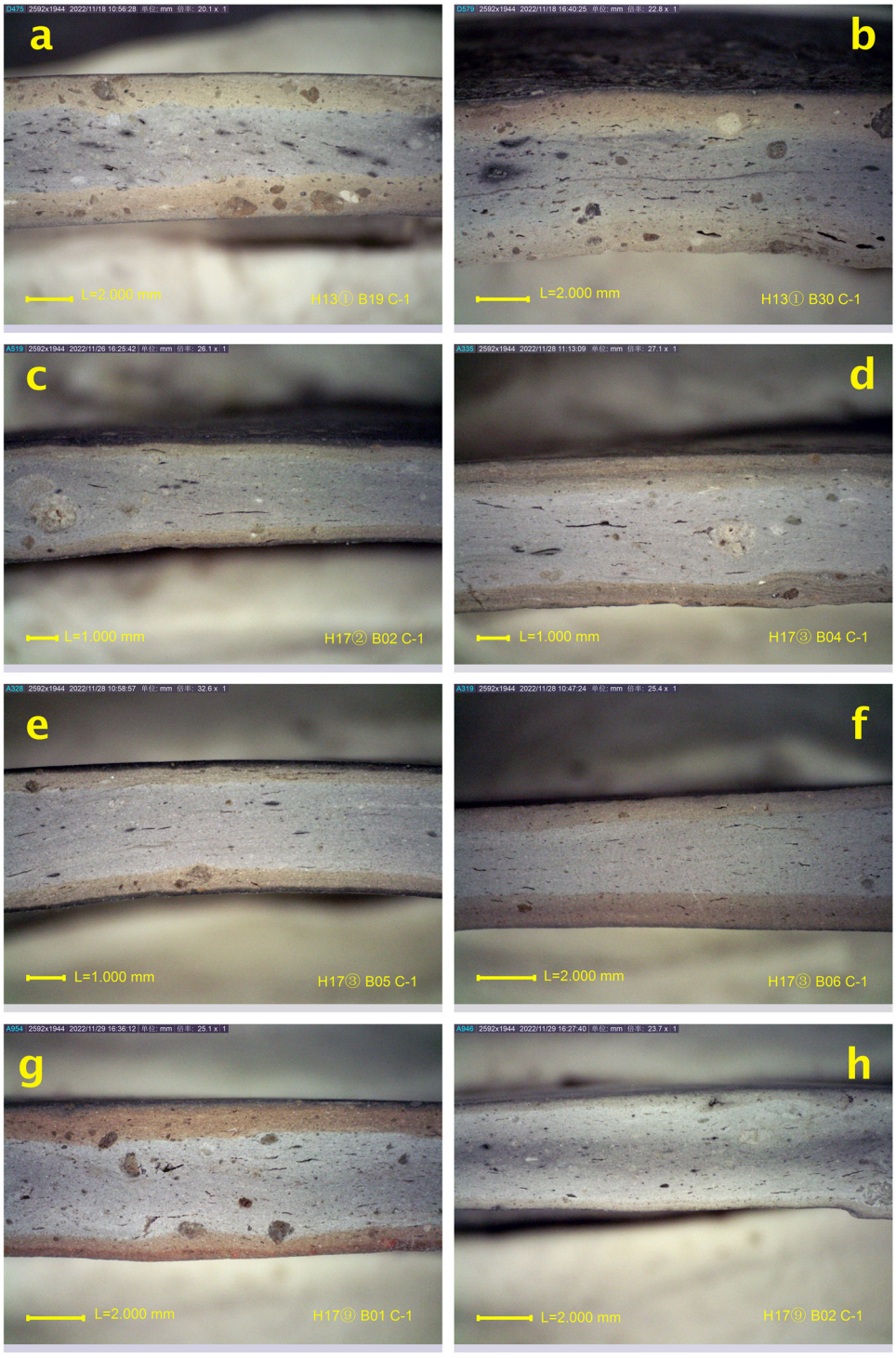

Figure 9: The cross-sections (a to h) of fine-paste sherds of the group BB*.

Despite the small sample size (n = 8), benchtop XRF results supported the delineation of groups AA, BB, and BB* by hhXRF data. Compared to group BB, group AA is characterized by higher Zr and Si but lower Rb, Al, and Ba. By contrast, group BB*, represented by sherd specimen FHZ091, clearly differs from groups AA and BB, especially in P, K, Ca, Sr, and Zn concentrations. We conclude that the fine-paste black pottery unearthed at Fenghuangzui is represented by three compositional groups (at the least).

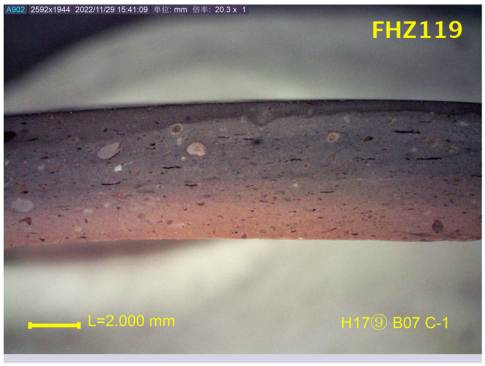

Figure 10: Cross-section of the sherd FHZ119 of group BB*.

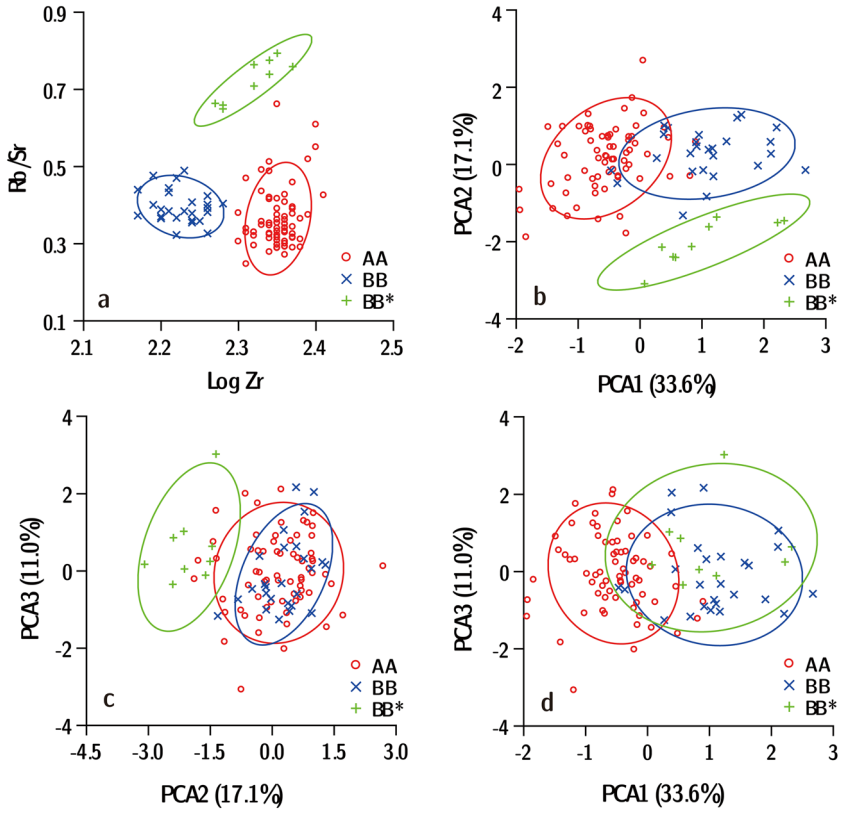

Figure 11: Scatter plots of the 103 fine-paste sherds (a) LogZr vs Rb/Sr; (b) PCA1 vs PCA2; (c) PCA2 vs PCA3; and (d) PCA1 vs PCA3, drawn with an 80% confidence ellipse.

4.4 Thin-Section Petrography

We selected the same eight sherds for thin-section petrography, and the results (Figure 14 and Table 4) show the types, sizes, and relative abundance of identifiable minerals.

Overall speaking, the eight sherds contain about the same types of minerals. The minerals in the clay matrix are mainly kaolinite and illite. Quartz and feldspar account for the non-plastic inclusions, whose particle sizes are usually smaller than 0.05 mm in diameter. A small quantity of mudstone (a fine-grained sedimentary rock) debris is present, with a particle size of 0.1–1 mm in diameter. All sherds contain a few pores, but the sherd specimen FHZ091 in group BB* has the most poorly developed pores (see Figure 9c for the microstructure of FHZ091).

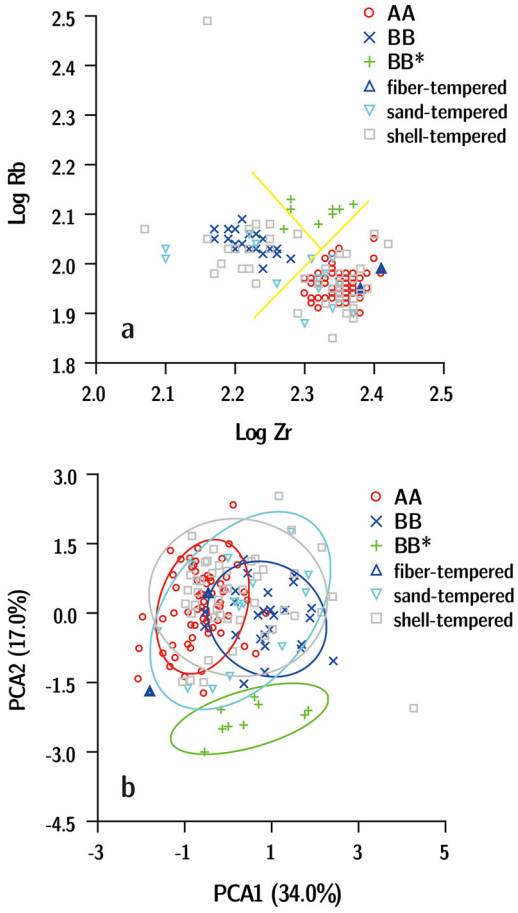

Figure 12: Scatterplot revealing (a) the similar patterning of chemical compositional variations with all sherds and (b) characterizing, again, the distinct chemical composition of group BB*.

However, groups AA, BB, and BB*, characterized by their chemical composition (Figures 11 and 12), differ in particle sizes and relative abundance of non-plastic inclusions. By calculating the ratio of kaolinite and illite to quartz and feldspar, we find out that sherds FHZ001, FHZ008, FHZ015, and FHZ102 of group AA have ratios less than 1; FHZ022, FHZ063, and FHZ080 of group BB have ratios greater than 1; and FHZ091 of group BB* has the ratio of nearly 1 (Figure 15).

In short, the thin-section petrographic results are compatible with the groupings of sherds based on microscopic examination and chemical composition, which once again confirms that the sherds were compositionally diverse. We also understand that the rough and coarse texture of sherds is primarily correlated with the particle sizes and relative abundance of non-plastic inclusions. This explains the significant chemical variations among different sub-groups.

Last but not least, we want to introduce the results of the thermal expansion analysis. Thermal expansion curves suggest that the six black pottery sherds were fired between 820 and 920°C. The sherd specimen FHZ100, assigned to group BB* chemically, was fired at 890°C. Overall, sherds of group BB were fired at higher temperatures than group AA's (Table 5). The firing temperature seems to differ slightly from the Upper Qujialing to Shijiahe periods, even though the sherd fired at the lowest temperature, FHZ145, dates to the Upper Qujialing period. We suggest that most black potteries unearthed at Fenghuangzui were fired between 820 and 920°C. Pottery kilns dating to the Shijiahe period were unearthed at Fenghuangzui in the 2020 and 2021 excavations (Li et al., 2022). Our Raman analysis and thermal expansion tests offer new information about how these kilns were used to produce black pottery. More discussions on this topic will be introduced in our following article.

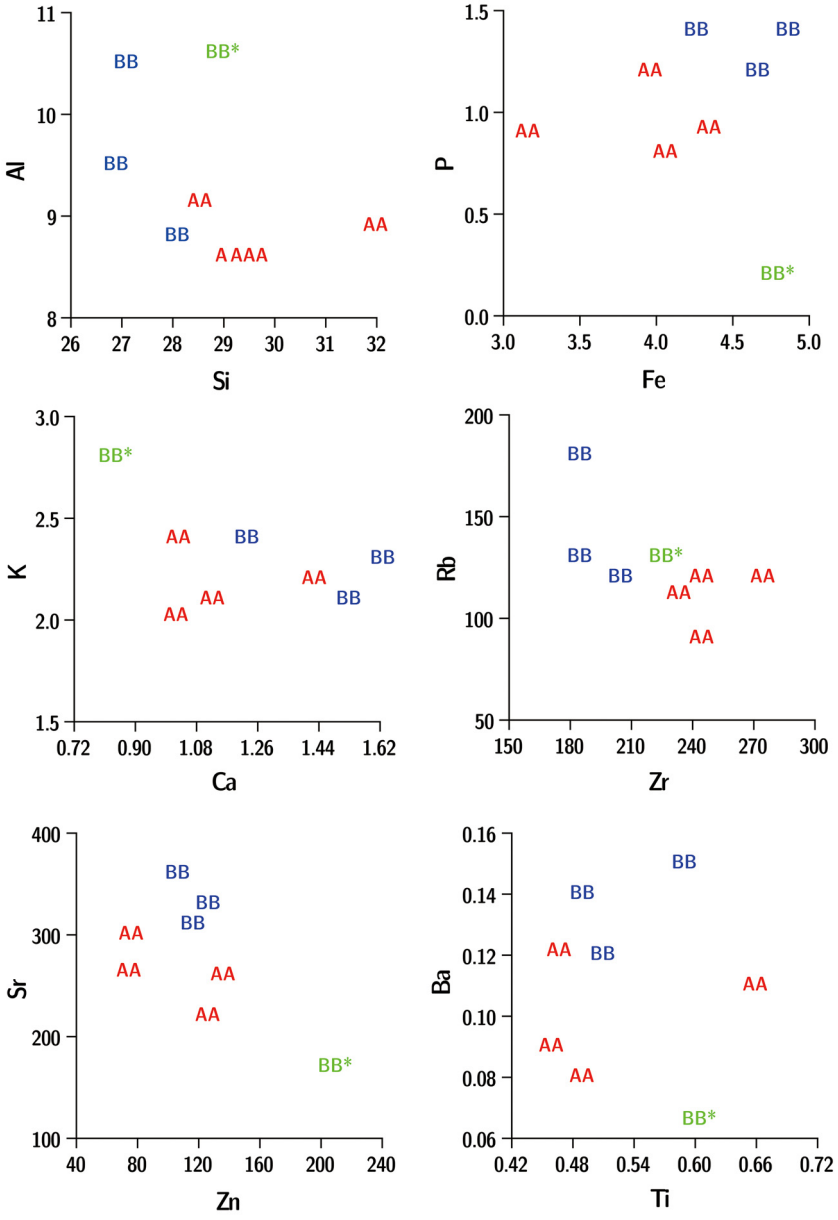

Figure 13: Scatter plots of elements in the eight sherds analyzed by benchtop XRF (Si, Al, Fe, P, Ca, K, Ti, and Ba, in wt%; Zr, Rb, Sr, and Zn, in ppm).

Table 3: Benchtop XRF results of the eight selected sherds

Compositional group	Sample	wt%										ppm			
		O	Si	Al	Fe	K	Ca	P	Na	Ti	Ba	Zr	Rb	Sr	Zn
AA	001	52.0	28.4	9.1	4.3	2.0	1.0	0.9	0.68	0.46	0.12	230	110	260	70
	008	52.3	29.2	8.6	3.9	2.1	1.1	1.2	0.73	0.45	0.09	240	90	260	130
	015	51.7	28.9	8.6	4.0	2.4	1.0	0.8	0.81	0.48	0.08	270	120	220	120
	102	49.2	31.8	8.9	3.1	2.2	1.4	0.9	0.86	0.65	0.11	240	120	300	70
BB	022	51.7	27.9	8.8	4.2	2.1	1.5	1.4	0.77	0.50	0.12	200	120	360	100
	063	50.5	26.9	10.5	4.8	2.4	1.2	1.4	0.52	0.48	0.14	180	180	310	110
	080	51.8	26.7	9.5	4.6	2.3	1.6	1.2	0.52	0.58	0.15	180	130	330	120
BB*	091	48.9	28.7	10.6	4.7	2.8	0.8	0.2	0.78	0.59	0.07	220	130	170	200

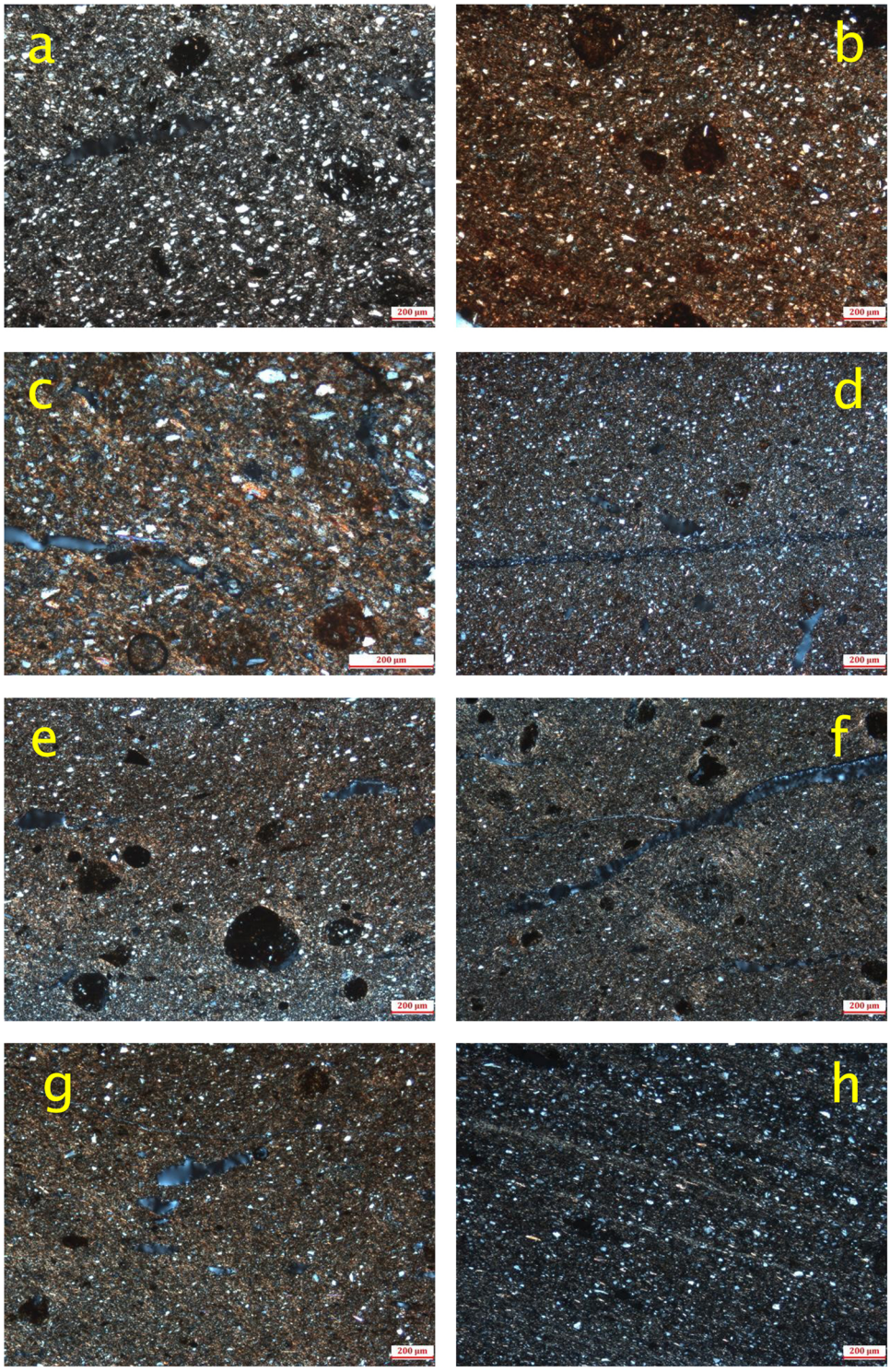

Figure 14: Thin-section petrography of the eight sherds. (a) FHZ001; (b) FHZ008; (c) FHZ015; (d) FHZ102; (e) FHZ022; (f) FHZ063; (g) FHZ080; and (h) FHZ091.

5 Discussion

Given the Raman identification of the black finish, microscopic examination, handheld and benchtop X-ray fluorescence analysis of sherds, and thermal expansion curves, we organize our discussions below around

Table 4: Thin-section petrographic results (CC = chemical composition, ME = microscopic examination)

Groups defined by CC	Subgroups defined by ME	Lab no.	Minerals and their particle sizes, and percentages			
AA	A	001	Kaolinite, Illite Particle size: <0.01 mm Percentage: 33%	Quartz, Feldspar Particle size: <0.05 mm Percentage: 60%	Mudrock Particle size: 0.2–1 mm Percentage: 5%	Pores Percentage: 2%
	A1	008	Kaolinite, Illite Particle size: <0.01 mm Percentage: 39%	Quartz, Feldspar Particle size: <0.05 mm Percentage: 55%	Mudrock Particle size: 0.1–0.4 mm Percentage: 5%	Pores Particle size: 0.2–1 mm Percentage: 1%
	A	015	Kaolinite, Illite Particle size: <0.01 mm Percentage: 37%	Quartz, Feldspar Particle size: <0.05 mm Percentage: 55%	Mudrock Particle size: 0.1–1 mm Percentage: 5%	Pores Particle size: 0.2–1 mm Percentage: 3%
	A1	102	Illite Particle size: <0.01 mm Percentage: 40%	Felsic Particle size: <0.02 mm Percentage: 55%	Mudrock Particle size: 0.1 mm Percentage: <1%	Pores Particle size: 0.1–0.5 mm Percentage: 3%
BB	A1/B	022	Kaolinite, Illite Particle size: 0.01 mm Percentage: 52%	Quartz, Feldspar Particle size: <0.05 mm Percentage: 40%	Mudrock Particle size: 0.1–0.3 mm Percentage: 5%	Pores Particle size: 0.2–2 mm Percentage: 3%
	A1/B	063	Kaolinite, Illite Particle size: 0.01 mm Percentage: 72%	Felsic Particle size: <0.01 mm Percentage: 25%	Mudrock Particle size: 0.1 mm Percentage: 1%	Pores Percentage: 1% Leakage: 2%
	B	080	Illite (dominant) Particle size: 0.01 mm Percentage: 60%	Felsic Particle size: <0.02 mm Percentage: 35%	Mudrock Particle size: 0.1–0.3 mm Percentage: <1%	Pores Particle size: 0.2–2 mm 5%
BB*	B	091	Illite (dominant) Particle size: 0.01 mm Percentage: 50%	Felsic Particle size: <0.05% Percentage: 50%	Mudrock Particle size: 0.1–0.2 mm Percentage: <1%	Pores Percentage: <1%

Figure 15: Line chart showing the varying ratios of (kaolinite + illite) to (quartz + feldspar) in the eight sherds.

Table 5: Firing temperatures determined for the eight selected sherds using the thermal expansion method (CC = chemical composition; N.A. = not available)

Sample no.	Ash pits	Period	Surface feature	Paste color on cross-section	Groups defined by CC	Firing temperature (°C)
FHZ009	H13	Shijiahe	Basket pattern	Reddish	AA	N.A.
FHZ017	H13	Shijiahe	Plain and burnished	Grayish	AA	920
FHZ093	H17	Shijiahe	Plain and burnished	Black	AA	840
FHZ100	H17	Shijiahe	Plain and burnished	Yellowish gray	BB*	890
FHZ118	H17	Shijiahe	Plain and burnished	Reddish gray	BB	N.A.
FHZ139	H17	Shijiahe	Plain and burnished	Grayish black	BB	850
FHZ145	H89	Upper Qujialing	Plain and burnished	Black	AA	820
FHZ147	H89	Upper Qujialing	Plain and burnished	Reddish black	BB	870

three topics: (1) the diversity of raw materials, (2) the temporal changes of raw materials, and (3) the technological choices as reflected by raw materials and vessel types and forms.

5.1 Diverse Clay Sources for Making Black Pottery

Raman's analysis of the black finish shows that carbon black is the colorant material. Microscopic examination reveals only a thin black layer on most sherds' surfaces, which may have been formed by the deposition and penetration of carbon particles into the pottery during or after the firing. There is no chemical evidence that the formation of a black finish was correlated with a particular type of clay.

Meanwhile, we learn from the microscopic examination and chemical compositional analysis that the 104 fine-paste sherds can be divided into 3 groups (AA, BB, and BB*). Group AA is characterized by sherds with a rough and coarse texture on the surface; by contrast, groups BB and BB* show a finer texture on the surface. Regarding chemical composition, group AA contains high Zr and low Rb; low Zr and high Rb characterize group BB; and group BB* contains a significantly lower concentration of Sr and a higher concentration of Rb than group BB. Principal component analysis confirms the compositional differences among the three groups and, especially, highlights the different chemical compositions of the BB* sherds. Thin-section petrography suggests that the three groups of sherds contain about the same types of clay minerals (kaolinite and illite, or illite only) and non-plastic inclusions (quartz, feldspar, and a small quantity of mudstone). However, the particle sizes and relative abundance of non-plastic inclusions seem to distinguish the three groups from one another, which, once again, is well explained by microscopic observations and chemical compositional variations.

Given the information above, we propose that three clay sources were used to make pottery, each characterizing a different group of pottery (AA, BB, and BB*). We consider "different clay sources" as another way of saying "different raw materials" and admit that "raw materials," as we use it here, is a generic term that broadly refers to the paste prepared by the potters working with the procured clay. In our study, some major and trace elements are better indicators of clay sources.

Zirconium (Zr) is among the few elements that help distinguish between groups AA and BB. Linear regression analysis suggests that the concentrations of Zr and Si, reported by benchtop XRF analysis, are positively correlated (R = 0.70, R^2 = 0.49). It is argued that as the particle size of the pottery-making raw material (clay) decreases, silicon (Si) concentration tends to decrease, yet that of zirconium (Zr) increases in the pottery produced from that specific clay (Beltrame et al., 2021). Our results suggest the opposite (a positive correlation between Si and Zr), probably because our sherds are mostly fine-paste and contain particle sizes of 63 μm or smaller. The dilution effect of more inclusions (quartz) must be minor. The differences in the concentrations of silicon and zirconium among the three groups should be explained by the relative abundance of quartz, feldspar, and probably zirconium silicate ($ZrSiO_4$) with smaller particle sizes. This explanation is also compatible with thin-section petrographic results.

Furthermore, zirconium is among the lithophile elements, and due to the strong resistance of ZrO_2 to weathering, its concentration is often used to evaluate the degree of soil weathering (Jackson, 1973). We suggest that the raw material (clay) of groups AA and BB should have differed in their degrees of weathering. The shell-tempered sherds are compositionally similar to the fine-paste sherds, and they can also be divided into groups AA and BB, indicating that the same two clay sources, with different degrees of weathering, were used to make the fine-paste and shell-tempered pots.

Although group BB* lies primarily in between groups AA and BB in terms of the concentration of zirconium, it is characterized by higher Rb and lower Sr, another two elements closely related to weathering (Dasch, 1969). In the process of soil formation, Sr is more active and easier to leach and migrate, while Rb is easy to be adsorbed by K-rich clays and easier to be enriched; thus, Rb/Sr ratio is often regarded as an important index to study paleoclimate and paleoenvironmental changes as well as to differentiate loess from paleosols (Chen et al., 1999, 2001). This implies that the clay used to make group BB* has a different geologic history. In addition, none of the shell-tempered, coarse-paste, and fiber-tempered pottery seemed to

demonstrate chemical compositional similarity to the fine-paste group BB*. This strengthens our argument that group BB* is produced from a distinct clay source (with a different geologic history). The uniqueness of group BB* is also confirmed by the distinct color of the cross-section of its sherds (Figures 9 and 10).

In short, we conclude that at least three clay sources were used to make the black pots unearthed from the three ash pits (H13, H17, and H89) at the Fenghuangzui site. These clay sources underwent varying degrees of weathering, suggesting that they may have been sourced from different localities or at different depths of the same loci. The 165 sherds contained similar mineral inclusions and were fired within the same temperature ranges, indicating consistency in tempering and firing practices. Given the discoveries of pottery kilns dating to the Shijiahe period at the site (Li et al., 2022), it is possible that the potters procured clays from the site and surrounding areas. However, more systematic surveys and sampling are needed to investigate this topic further.

5.2 Temporal Changes in the Procurement of Clay

The 165 sherds were sampled from 3 ash pits (H13, H17, and H89) that differed in their date of formation. This allows us to explore the production of black pottery through diachronic and synchronic perspectives.

First, sherds unearthed from the three ash pits largely overlap in their chemical compositions, implying that the clay sources for making black pottery were neither restricted to the users of a given ash pit nor varied significantly through time. The same clay sources were consistently used from the Upper Qujialing period to the Shijiahe period.

Second, each ash pit contains black pottery that can be divided into groups AA and BB. The coexistence of groups AA and BB suggests that different clay sources were used simultaneously, and this practice continued for an extended period.

Nevertheless, differences do exist among the ash pits. For example, ash pit H17 contains a much higher proportion of pottery characterized by groups BB and BB* than ash pit H13, which, we suggest, is related to the different functional or contextual uses of H17. According to our count of the excavated sherds, H17 contains more serving and drinking vessels than H13 (Figure 3c). Meanwhile, H17 contains thin-walled painted pottery and abundant animal and plant remains related to feasts at the household or community level (Table 6). H17 demonstrates the most substantial evidence of feasts involving consuming more food (meat) and drinks. In addition, ash pit H89 is dated the earliest among the three pits, and most sherds from H89 are divided into group AA, only a few into group BB, and rarely into group BB*. Even though the users of all three ash pits accessed the three clay sources, the older one seemed to have relied heavily on group AA while the two younger ones exploited the clay sources characterized by group BB and BB* more intensively.

To summarize, despite the overall consistency of the clay sources, there is a temporal variation in the degree of exploitation of the different clay sources. We propose that the exploitation of finer clay sources (BB and BB*) and the more intensive consumption of protein foods and liquids be correlated. Both played a role in strengthening social cohesion and making Fenghuangzui an attractive place to live.

5.3 The Potters' Technological Choices

It turns out that within each ash pit, different clay sources, instead of a single one, were used to make black pots at the site of Fenghuangzui. We argue that the Neolithic potters at Fenghuangzui must have decided to do so purposefully. We base our arguments mainly on two lines of evidence.

First, observations of complete pottery and sherds with recognizable shapes and forms suggest a correlation between surface decoration and vessel shape and form. For example, black pottery with a basket pattern often belongs to large vessels such as *guan*-jars and *ding*-tripods, as well as to some *bo*-bowls and vessel lids, while most serving and drinking vessels such as *wan*-bowls, *bo*-bowls, *dou*-stemmed bowl, *pan*-plate, and *hu*-

Table 6: Artifactual remains unearthed from the three ash pits (serving vessels include *wan*-bowls, *bo*-bowls, *dou*-stemmed bowls, *pan*-plates, *die*-saucers, and vessel lids; drinking vessels include *hu*-jars, *bei*-cups, and *gui*-tripod pitchers. N.A. = not available)

Ash pit	Faunal remains	Chemical compositions of black pottery			Count of serving and drinking vessel sherds
		AA	BB	BB*	
H89	N.A.	8 (80%)	2 (20%)	0	N.A. (two restored *bo*-bowls)
H17	1,869 skeletal remains, with 553 identifiable specimens, of which 334 belong to mammals and 224 to pigs. The minimum number of mammal individuals is 37, with 12 being pigs, and 9 medium-sized deer	21 (48%)	16 (36%)	7 (16%)	672 (55%)
H13	230 skeletal remains, with 73 identifiable specimens, of which 53 belong to pigs, and the minimum number of individuals is 10, with 5 being pigs	39 (80%)	8 (16%)	2 (4%)	251 (30%)

jar are plain or polished. This correlation is also reflected in the statistics of pottery sherds, with H17 having more food and drink vessels and also containing more plain or polished sherds and H13 having a higher proportion of *guan*-jars and *ding*-tripods and thus more sherds with a basket pattern (Figure 4b and c). Figure 8d shows that most sherds with a basket pattern fall within the chemical compositional variations characterized by group AA, corresponding to a source of clay most widely or easily available. In contrast, groups BB and BB* consist mainly of plain or burnished surfaces. We suggest that the potters made large storage vessels with a basket pattern from the clay characterizing group AA more intensively; meanwhile, they used the clay characterizing groups BB and BB* to produce serving and drinking vessels (*dou*-stemmed bowl, *pan*-plate, *wan*-bowl, and *hu*-jar). The serving and drinking vessels were also produced from the clay characterizing group AA, possibly due to its easy or great availability.

Second, the clay used to make pottery for group BB* is unique in its chemical composition. Its use was restricted to fine-paste pots. The potters did not make shell-tempered, coarse-paste, or fiber-tempered pots from this type of clay. Meanwhile, the pottery of group BB* shows a light yellowish-gray color on the cross-section, which differs from groups AA and BB. This implies that the color of the used clay may also be lighter or somehow unusual. Clay's color is the main criterion for modern Mayan potters to recognize the quality of the clay, and good clay in Ticul is yellow or white, available only at specific locations (Arnold, 1971). We then propose that the Fenghuangzui potters should have understood the differences among the clays and that they chose some clay sources over others depending on their needs. Furthermore, the phosphorus concentration is extremely low in FHZ091 (P, 0.2, P_2O_5, 0.44, in wt%), a sherd specimen of group BB* with a dense texture and fewer pores, possibly indicating the intentional use of the clay and/or a particular function of use (e.g., Heron & Evershed, 1993; Rodrigues & da Costa, 2016). Although more samples are needed to evaluate this possibility, we believe that this highlights the potter's preference for using some raw materials over others in making certain black pots. How, then, did the potters make their decisions?

We learn from many ceramic ethnoarchaeological and experimental studies that clay's physical and chemical properties are crucial to pottery-making. For instance, the potter must consider the clay's plasticity to ensure that it can be worked with in various ways and that its properties are good enough to be dried and fired as desired (Bronitsky, 1986). The finer clay particles usually make the clay more plastic, causing the pots to have a greater shrinkage rate after drying and firing (Liu, 1990). Groups BB and BB* were made from finer clays, which must have a greater shrinkage rate, high plasticity, and take longer to dry. The chances are higher that pots made from this type of clay crack when fired. Therefore, the finer clays are not suitable, or cannot be used, for making large pots such as *guan*-jar for storage purposes. Neither were the finer clays preferred to make common vessels considering the greater investment of labor and time. By contrast, we propose that the clays for making pots of group AA must have been widely available and workable. They required less time and effort to procure and process, making them ideal for larger or more common and rough vessels.

From the consumers' perspective, people often choose a particular type of pot because of the pot's hardness, strength, water permeability, texture, and visual effects. The choice of clay is crucial to the performance and life history of the pottery from the beginning. First, producing pots from finer clays will result in a higher degree of hardness (Liu, 1990) and high strength (Kirchner, 1979). Additionally, the size and structure of clay particles were determinants of the pores (e.g., Hein et al., 2008; Maggetti & Rossmainith, 1981). The finer clay results in smaller pores, significantly reducing the chance of water leaking. The permeability test suggests that "real" black pottery has better impermeability (Fan, 2015). We suggest that this may also be related to the particle size of the sherds, but further experiments are needed to verify this. Last but not least, the body, once burnished on the surface, will also reduce the chance of water leaking (Fan et al., 2005), and at the same time, the finer clays and burnished surface will produce the pots with a great texture and make them visually appealing. In short, we suggest that the potters at Fenghuangzui must have chosen finer clays for making serving and drinking vessels for a high degree of hardness and better water resistance, physical strength, textures, and visual effects.

To summarize the information above, we suggest that while producing black pots, the Fenghuangzui potters chose particular types, or sources, of clays intentionally and that their technological choices of different clays were influenced not only by the accessibility and workability of raw materials but also by the desires for superior quality and functions.

6 Concluding Remarks

In addition to the techno-functional properties, social and economic considerations must have driven the potters to look for and procure the clays that better served their consumers' social needs. Our case study focused on 165 Neolithic black pottery sherds unearthed from the site of Fenghuangzui in the Xiangyang City of Hubei Province, central China. The sherds are mainly dated from the Late Upper Qujialing to the Late Shijiahe period and are characterized by three clay sources (AA, BB, and BB*).

We noticed that the pottery of groups BB and BB* mainly belonged to the ash pit H17 and was used to serve foods and liquids. Other archaeological evidence suggests that ash pit H17 was related to feasting activities. Under this context, pottery was not only produced for daily use but also assigned symbolic meanings. The manufacture of (black) pots with enhanced resistance to water leaking, a higher degree of hardness, better physical strength, great texture, and visual effects served to meet the needs of social behaviors for exhibition. Meanwhile, pots with burnished surfaces and those produced from finer, or even unique, clays (such as those of group BB*) symbolized access to limited resources, higher technological levels, and labor investment. The users' economic wealth, social status, or community identity were contextualized within these black pots. We believe that the complexity and diversity of the Fenghuangzui black pots not only disclose the potters' technological choices but also, more importantly, serve as material representations of the involvement of the Fenghuangzui inhabitants in significant social and political events.

Acknowledgments: We thank Mrs. Ye Ma from the Public Service Platform for Scientific Research of Wuhan University for performing the benchtop XRF analysis. We also thank the anonymous reviewers for their constructive comments and suggestions, which have strengthened the logic and clarity of our arguments.

Funding information: The work was financed by the National Youth Talent Support Program (grant number 1105-212200003, granted to Tao Li).

Author contributions: All authors have accepted responsibility for the entire content of this manuscript and approved its submission. TL, GL, and SS conceived the study and were significant contributors to the writing of the manuscript. HT and SS conducted the pottery typological analysis and prepared Figures 1–3. GL and TL performed the XRF and Raman analyses and analyzed and interpreted the data. JZ and QL carried out the thermal expansion tests.

Conflict of interest: The authors state no conflict of interest.

Data availability statement: All data generated during this study are included in this published article and its supplementary information files.

References

An, Z. (1979). The Neolithic archaeology of China a brief survey of the last thirty years. *Early China*, *5*, 35–45.

An, Z. (1988). Archaeological research on Neolithic China. *Current Anthropology*, *29*(5), 753–759.

Ao, X., He, L., Shao, J., Wu, J., & Li, T. (2023). Handheld X-ray fluorescence analysis of pottery unearthed from the site of Xinjie in Shaanxi Province of Northern China. *Asian Archaeology 7*, 63–80. doi: 10.1007/s41826-41023-00068-41822.

Arnold, D. E. (1971). Ethnomineralogy of Ticul, Yucatan potters: Etics and emics. *American Antiquity 36*, 20–40.

Bell, I. M., Clark, R. J., & Gibbs, P. J. (1997). Raman spectroscopic library of natural and synthetic pigments (pre-1850 AD). *Spectrochimica Acta Part A: Molecular and Biomolecular Spectroscopy*, *53*, 2159–2179.

Beltrame, M., Sitzia, F., Arruda, A. M., Barrulas, P., Barata, F. T., & Mirão, J. (2021). The Islamic ceramic of the Santarém Alcaçova: Raw materials, technology, and trade. *Archaeometry*, *63*, 1157–1177.

Bronitsky, G. (1986). The use of materials science techniques in the study of pottery construction and use. *Advances in Archaeological Method and Theory*, *9*, 209–276.

Chen, J., An, Z., & Head, J. (1999). Variation of Rb/Sr ratios in the Loess-paleosol sequences of central China during the last 130,000 years and their implications for Monsoon paleoclimatology. *Quaternary Research*, *51*(3), 215–219. doi: 10.1006/qres.1999.2038.

Chen, J., Wang, Y., Chen, Y., Liu, L., Ji, J., & Lu, H. (2001). Rb and Sr geochemical characterization of the Chinese Loess and its implications for Palaeomonsoon climate. *Acta Geologica Sinica*, *75*, 259–266.

Childe, V. G. (1937). Neolithic black ware in Greece and on the Danube. *The Annual of the British School at Athens*, *37*, 26–35. doi: 10.1017/S0068245400017949.

Cui, J., Zhang, W., Tian, H., & Zhao, Y. (2017). Heilongjiang Youyixian Fenglinchengzhi chutu heiyi taopian ji yanliaokuai de kexue fenxi (Scientific investigations of black slipped pottery fragments and pigments unearthed from the Fenglin Ancient City in Youyi County, Heilongjiang Province). *Beifang Wenwu* (Cultural Relics of Northern China), *2017*(3), 48–51 (in Chinese with English abstract).

Dasch, E. J. (1969). Strontium isotopes in weathering profiles, deep-sea sediments, and sedimentary rocks. *Geochimica et Cosmochimica Acta*, *33*, 1521–1552.

Druc, I., Underhill, A., Wang, F., Luan, F., & Lu, Q. (2018). A preliminary assessment of the organization of ceramic production at Liangchengzhen, Rizhao, Shandong: Perspectives from petrography. *Journal of Archaeological Science: Reports*, *18*, 222–238.

Du, Z. (1982). Shilun Longshan wenhua de danketao (Egg-shelled black pottery of the Longshan culture). *Kaogu* (Archaeology), *1982*(2), 176–181 (in Chinese with English abstract).

Fan, D., Luan, F., Fang, H., Yu, H., Cai, F., & Wen, D. (2005). Shandong Rizhaoshi Liangchengzhen Longshan wenhua taoqi de chubu yanjiu (Preliminary study of the Longshan culture pottery from the Liangchengzhen in Rizhao City, Shandong Province). *Kaogu* (Archaeology), *2005*(08), 65–73, 102 (in Chinese with English abstract).

Fan, Z. (2015). *Changjiang Zhongxiayou Nizhiheitao De Qiyuan Yu Fazhan* (Origin and development of fine-paste black pottery in the Middle and Lower Yangtze River valley). (Master thesis). Zhongshan University (in Chinese with English abstract).

Fanti, L., Melosu, B., Cannas, C., & Mameli, V. (2024). Pottery vessels and technology of "colouring materials" in the central-western Mediterranean (Sardinia, Italy) during the Middle Neolithic: An interdisciplinary approach combining use-wear and chemical-physical analysis. *Journal of Archaeological Science: Reports*, *53*, 104321. doi: 10.1016/j.jasrep.2023.104321.

Fu, S., Li, J., Dong, Z., Liang, S., Wu, J., Guo, B., & Liu, Y. (1934). *Chengziya: Shandong Licheng Longshanzhen Zhi Heitao Wenhua Yizhi*. Zhongyang Yanjiuyuan Lishiyuyan Yanjiusuo (in Chinese).

He, L., Yao, S., Sun, Z., Shao, J., Di, N., & Li, T. (2023). Ceramic raptors unearthed at the site of Shimao (2300–1800 BCE) in northern China: Production and use. *Journal of Archaeological Science: Reports*, *48*, 103844. doi: 10.1016/j.jasrep.2023.103844.

Hein, A., Müller, N. S., Day, P. M., & Kilikoglou, V. (2008). Thermal conductivity of archaeological ceramics: The effect of inclusions, porosity and firing temperature. *Thermochimica Acta 480*, 35–42. doi: 10.1016/j.tca.2008.09.012.

Heron, C., & Evershed, R. P. (1993). The analysis of organic residues and the study of pottery use. In M. B. Schiffer (Ed.), *Archaeological method and theory* (Vol. 5, pp. 247–284). University of Arizona Press.

Holmberg, E. J. (1964). The appearance of Neolithic black burnished ware in mainland Greece. *American Journal of Archaeology*, *68*, 343–348.

Hubei (Hubei Provincial Institute of Cultural Relics and Archaeology). (2001). *Yidu Chengbeixi* (The Chengbeixi Site in Yidu). Wenwu Chubanshe. (In Chinese).

Jackson, M. L. (1973). *Soil chemical analysis*. Prentice Hall of India Pvt. Ltd.

Kirchner, H. P. (1979). *Strengthening of ceramics: Treatments, tests, and design applications*. Marcel Dekker Inc.

Łaciak, D., Borowski, M. P., Łydżba-Kopczyńska, B., Baron, J., & Furmanek, M. (2019). Archaeometric characterisation and origin of black coatings on prehistoric pottery. *Geochemistry*, *79*(3), 453–466. doi: 10.1016/j.chemer.2019.07.004.

Li, J., Chen, X., Deng, Z., & Gu, Z. (1979). Hemudu yizhi taoqi de yanjiu (A study of the pottery unearthed at Hemudu). *Guisuanyan Xuebao (Journal of the Chinese Ceramic Society)*, *7*(2), 105–112.

Li, P., Hu, Y., Zhang, X., Zhang, C., Chu, X., & Li, T. (2024). Chemical variations of clays and pottery within a relatively small spatial extent: Initial insights from modern pottery-making in Central China. *Archaeological Research in Asia*, *38*, 100504. doi: 10.1016/j.ara.2024.100504.

Li, T. (2016). *Economic differentiation in Hongshan core zone communities (northeastern China): A geochemical perspective*. (Ph.D. dissertation). University of Pittsburgh.

Li, T. (2020). Shiqian taoqi de shouchishi x shexian yingguang guangpu fenxi (Compositional analysis of prehistoric Chinese pottery with handheld X-ray fluorescence (hhXRF) analyzer). *Nanfang Wenwu* (Cultural Relics of South China), *2020*(3), 268–276.

Li, T., Li, G., Li, Z., Wu, T., Tian, H., Shan, S., & Wang, L. (2022). Surface treatment of red painted and slipped wares in the middle Yangtze River valley of Late Neolithic China: Multi-analytical case analysis. *Heritage Science*, *10*, 188. doi: 10.1186/s40494-022-00824-0.

Li, T., Li, P., Song, H., Xie, Z., Fan, W., & Lü, Q. Q. (2022). Pottery production at the Miaodigou site in central China: Archaeological and archaeometric evidence. *Journal of Archaeological Science: Reports*, *41*, 103301. doi: 10.1016/j.jasrep.2021.103301.

Li, T., Yao, S., He, L., Yu, X., & Shan, S. (2021). Compositional study of household ceramic assemblages from a Late Neolithic (5300–4500 cal BP) earthen walled-town in the middle Yangtze River valley of China. *Journal of Archaeological Science: Reports 39*, 103159. doi: 10.1016/j.jasrep.2021.103159.

Li, W. (1994). Jingshan Qujialing yizhi disanci fajue yicun de zhitao gongyi he niandai wenti (Pottery-making technology and chronology of the pottery artifacts from the third excavation at the Qujialing site in Jingshan County). *Zhongguo Lishibowuguan Guankan* (Journal of National Museum of China), *1994*(1), 16–23 (in Chinese).

Li, W., & Huang, S. (1985). Qianshuo Daxi wenhua taoqi de shentan gongyi (Penetration of carbon on the daxi culture black pottery). *Jianghan Kaogu* (Jianghan Archaeology), *1985*(4), 46–51 (in Chinese with English abstract).

Liu, K. (1990). *Taoci Gongyi Yuanli* (Principles in Pottery-making Technologies). Huanan Ligong Daxue Chubanshe (South China University of Technology Press).

Longacre, W. A., Xia, J., & Yang, T. (2000). I want to buy a black pot. *Journal of Archaeological Method and Theory*, *7*, 273–293.

Lu, Q. (2021). Jinan Zhangqiuqu Longshanzhen heitao zuofang de renleixue diaocha (Black pottery-making workshops in Longshan Town of Zhangqiu District, Jinan City of Shandong Province). *Dongfang Kaogu* (Cultural Relics of Northern China), *18*, 345–358 (in Chinese).

Lu, X., Li, W., Liu, B., & Li, X. (2013). Liangzhu Gucheng Yizhi taoqi de fenxi yanjiu (Technical examinations of pottery artifacts unearthed from the Liangzhu Ancient City). *Zhongguo Kexue: Jishu Kexue* (Science China Technological Sciences), *43*, 460–466 (in Chinese).

Lu, X., Li, W., Luo, H., He, N., & Li, X. (2011a). Taosi yizhi Longshan Shidai heise taoyi de yanjiu (Study of the Longshan Culture black pottery from the Taosi Site). *Zhongguo Kexue: Jishu Kexue* (Science China Technological Sciences), *41*, 906–912 (in Chinese).

Lu, X., Li, W., Luo, H., He, N., & Li, X. (2011b). The black pottery coating of Longshan times from Taosi site. *Science China Technological Sciences*, *54*(7), 1708–1714. doi: 10.1007/s11431-011-4439-4.

Maggetti, M., & Rossmainith, M. (1981). Archaeothermometry of kaolinitic clays. *Revue d'Archéométrie*, *1*, 185–194.

Meng, H. (1997). *Changjiang Zhongyou Shiqian Wenhua Jiegou* (Structures and Systems of the Neolithic Cultures in the Middle Yangtze River Valley). Changjiang Wenyi Chubanshe (in Chinese).

Nam, S., Walsh, R., & Lee, G. A. (2020). Innovation, imitation, and identity: Mayeon black ware and social complexity in Southwestern Korea. *Archaeological Research in Asia*, *23*, 100197. doi: 10.1016/j.ara.2020.100197.

Oikonomou, A., Papachristodoulou, C., Gravanic, K., Stamoulis, K., & Ioannides, K. (2012). Black- and red-slipped pottery from ancient Cassope (NW Greece): Inference of provenance and production technology based on a multi-analytical approach. *Proceedings of the 39th International Symposium for Archaeometry* (pp. 251–256).

Qiu, P., Wang, C., Li, F., Zhou, G., Ren, S., Chen, X., & Liang, Z. (2001). Dawenkou Longshan Wenhua heitao nei tanxianwei de chubu yanjiu (initial study on carbon fibers in the black pottery of the Dawenkou and Longshan Cultures). *Ziran Kexueshi Yanjiu* (Studies in the History of Natural Sciences), *20*(1), 79–83 (in Chinese with English abstract).

Rodrigues, S. F. S., & da Costa, M. L. (2016). Phosphorus in archeological ceramics as evidence of the use of pots for cooking food. *Applied Clay Science*, *123*, 224–231.

Shan, S. (2018). *Qujialing Wenhua Yanjiu* (A Study on the Qujialing Culture). (Ph.D. dissertation). Wuhan University (in Chinese).

Shan, S. (2021). Qujialing Xiaceng Wenhua de jieding, shkong jiegou, ji xiangguan wenti (The Lower Qujialing Culture: Definition, spatial-temporal distribution, and related issues). *Sichuan Wenwu* (Sichuan Cultural Relics), *2021*(4), 29–42.

Shan, S., He, L., Yao, S., Wang, J., Yu, X., & Li, T. (2021). The emergence of walled towns in prehistoric middle Yangtze River valley: Excavations at the Zoumaling site. *Archaeological Research in Asia*, *26*, 100285. doi: 10.1016/j.ara.2021.100285.

Shen, J., Zhai, J., Li, C., & Zhang, L. (2008). Longshan heitao xianwei jiegou fenxi he shentan gongyi yanjiu (Microstructural examination and carbon smudging of the Longshan culture black pottery). *Zhongguo Taoci* (China Ceramics), *2008*(3), 43–45 (in Chinese with English abstract).

Shimada, I., & Wagner, U. (2019). Technology and organization of black pottery production on the north coast of Peru. *Boletín de Arqueología PUCP*, *27*, 133–156.

The Jingzhou Museum, Peking University, Hubei Provincial Institute of Cultural Relics and Archaeology, The Shijiahe Archaeological Team. (2011). *Tanjialing* (The Tanjialing Site). Wenwu Chubanshe (in Chinese).

Trąbska, J., Wesełucha-Birczyńska, A., Zięba-Palus, J., & Runge, M. T. (2011). Black painted pottery, Kildehuse II, Odense County, Denmark. *Spectrochimica Acta Part A: Molecular and Biomolecular Spectroscopy*, *79*(4), 824–830. doi: 10.1016/j.saa.2010.08.068.

Tsurev, A. (2022). Black is always in fashion: Early production of Dark Burnished Ware in the Neolithic of Upper Thrace. *Studia Praehistorica*, *16*, 11–32. doi: 10.53250/stprae16.11-32.

Underhill, A. P. (1991). Pottery production in chiefdoms: The Longshan period in Northern China. *World Archaeology*, *23*(1), 12–27.

Wang, F., & Zhou, G. (2003). *Zigui Liulinxi* (The Liulinxi Site in Zigui). Kexue Chubanshe (in Chinese).

Wang, W., Fu, L., Huang, Y., & Xu, W. (2023). Compositional analysis of black-slipped pottery from the Hulushan and Maoershan kiln sites: Insights into social complexity in northern Fujian. *Journal of Archaeological Science: Reports*, *51*, 104149. doi: 10.1016/j.jasrep.2023.104149.

Wang, W., & Zhang, C. (1993). Hunan Linlixian Hujiawuchang xinshiqi shidai yizhi (The Neolithic Hujiawuchang site in Linli County of Hunan Province). *Kaogu Xuebao* (Acta Archaeologica Sinica), *1993*(2), 171–206, 281–284 (in Chinese).

Wu, G. D. (1930). *Pingling Fangguji* (A Visit to Pingling). Zhongyang Yanjiuyuan Lishi Yuyan Yanjiusuo (Bulletin of the Institute of History and Philology Academia Sinica) (in Chinese).

Wu, G. D. (1938). *Prehistoric Pottery in China*. The Courtauld Institute of Art.

Xiao, R., Luo, Y., Tao, Y., Zhang, D., & Cui, J. (2022). Qujialing yizhi shiqian heiyou danketao yanjiu (Scientific analysis of the black slipped pottery unearthed from the Qujialing site). *Jianghan Kaogu (Jianghan Archaeology)*, *2022*(2), 114–122.

Yiouni, P. (2001). Surface treatment of Neolithic vessels from Macedonia and Thrace. *The Annual of the British School at Athens*, *96*, 1–25.

Zhang, X. (1987). Jianghan dongbu diqu xinshiqi shidai wenhua chulun (Initial insights into the Neolithic cultures in the Eastern Jianghan Plain). *Kaogu Yu Wenwu* (Archaeology and Cultural Relics), *1987*(4), 56–66 (in Chinese).

Zhang, X., He, D., & Wang, Y. (1982). Shilun Daxi wenhua taoqi de tedian (Characteristics of the Daxi culture pottery). *Jianghan Kaogu* (Jianghan Archaeology), *1982*(2), 13–19, 92, 113 (in Chinese).

Zhong, H. (1989). Dawenkou: Longshan Wenhua Heitao Gaobingbei de Moni Shiyan (Dawenkou: Experimental Studies on the Black High-footed Cups). In B. Su (Ed.), *Kaoguxue Wenhua Lunji er* (Collections of Papers on Archaeological Cultures, Vol. II, pp. 255–273). Wenwu Chubanshe (in Chinese).